The Astrophysical Journal, 635:L169–L172, 2005 December 20

FIRST OPTICAL IMAGES OF CIRCUMSTELLAR DUST SURROUNDING THE DEBRIS DISK CANDIDATE HD 32297

Paul Kalas[1,2]

Received 2005 October 17; accepted 2005 November 17; published 2005 December 6

ABSTRACT

Near-infrared imaging with the *Hubble Space Telescope* recently revealed a circumstellar dust disk around the A star HD 32297. Dust-scattered light is detected as far as 400 AU radius, and the linear morphology is consistent with a disk ~10° away from an edge-on orientation. Here we present the first optical images that show the dust-scattered light morphology from 560 to 1680 AU radius. The position angle of the putative disk midplane diverges by ~31°, and the color of dust scattering is most likely blue. We associate HD 32297 with a wall of interstellar gas and the enigmatic region south of the Taurus molecular cloud. We propose that the extreme asymmetries and blue disk color originate from a collision with a clump of interstellar material as HD 32297 moves southward, and discuss evidence consistent with an age of 30 Myr or younger.

Subject headings: circumstellar matter — stars: individual (HD 32297)

1. INTRODUCTION

Debris disks are the exosolar analogs of our zodiacal light and Kuiper Belt, and each new discovery represents an opportunity to understand how planetary systems form and evolve around other stars. Schneider et al. (2005) recently showed that HD 32297, an A star at $\sim 112^{+15}_{-12}$ pc, illuminates a dusty nebulosity resembling the edge-on debris disks around β Pic (Smith & Terrile 1984) and AU Mic (Kalas et al. 2004). HD 32297 was one of 26 stars that they identified as debris disk candidates for coronagraphic imaging with the NICMOS camera aboard the *Hubble Space Telescope*. Using the F110W filter ($\lambda_c = 1104$ nm, $\Delta\lambda = 592$ nm), the HD 32297 disk was found to be extended by at least 400 AU (3.″3) to the northeast with P.A. = 47.°6 ± 1° (G. Schneider, 2005, private communication), and at least 250 AU to the southwest. The hundreds of AU extent of the disk, and the significant asymmetry, are indeed comparable to those of β Pic (Kalas & Jewitt 1995). Here we present new *R*-band observations of HD 32297 using a ground-based coronagraphic camera that reveal a larger and more asymmetric circumstellar nebulosity than shown by the *HST* data.

2. OBSERVATIONS AND DATA ANALYSIS

We artificially eclipsed HD 32297 using an optical stellar coronagraph at the University of Hawaii 2.2 m telescope on Mauna Kea, Hawaii (Kalas & Jewitt 1996). Data were acquired with a Tek 2048 × 2048 CCD with a scale of 0.″407 pixel^{-1} and through a standard broadband *R* filter ($\lambda_c = 647$ nm, $\Delta\lambda = 125$ nm). Observations were made on 2005 September 28, with a 6.″5 diameter occulting spot and 1320 s effective integration time. Measurements of photometric standard stars showed photometric condition, with image quality, as measured by the FWHM of field stars, equal to ~1.″2. A series of short, unocculted integrations yielded $R = 7.9 \pm 0.1$ mag for HD 32297. We also observed three other bright stars with the coronagraph to check for spurious features such as diffraction spikes and internal reflections.

After the data were bias subtracted, flat-fielded, and sky-subtracted, we subtracted the stellar point-spread function (PSF) to remove excess stellar light from around the occulting spot. We used the real PSFs from other stars observed throughout each night, as well as artificial PSFs. Artificial PSF subtraction is effective for HD 32297 because the circumstellar disk is close to edge-on. We extracted the stellar PSF for each image of HD 32297 by sampling the image radially in a direction perpendicular to the P.A. of the disk. We then fit a polynomial to the data and generated an artificial PSF that is a figure of rotation of the polynomial. The PSFs were then scaled and registered to each data frame such that subtraction minimized the residual light in directions perpendicular to the disk beyond the edge of the occulting spot.

3. RESULTS

Figure 1 presents our *R*-band image of nebulosity surrounding HD 32297. The inner detection limit is 5.″0, and the nebulosity is detected as far as 15″ (1680 AU) radius. On these spatial scales the two ansae taken together do not resemble a circumstellar disk because the apparent midplanes diverge in position angle. Instead the curved morphology resembles that of pre–main-sequence stars such as SU Aur and Z CMa (Nakajima & Golimowski 1995). The northeast side is a relatively narrow structure resembling the near edge-on disk described by Schneider et al. (2005), but with P.A. = 34° ± 1° that is 13.°6 smaller than that measured in the *HST* NICMOS data. The southwest side of the nebulosity is a broader structure that curves westward with radius. We adopt P.A. = 245° ± 2°, which is 18° away from the midplane P.A. measured by Schneider et al. (2005), and forms a 31° angle with the northeast midplane in our data. The FWHM of the disk perpendicular to the midplane at 8″ radius is 3.″7 and 5.″0 for the northeast and southwest sides, respectively.

The midplane radial surface brightness profiles for the southwest side is 0.3–0.5 mag arcsec^{-2} brighter than the northeast side between 5″ and 10″ radius, and approximately equal further out (Fig. 2). PSF subtraction dominates the uncertainty in the absolute flux measurements, but the relative flux measurements between the northeast and southwest sides remain constant between different PSF subtractions. The cumulative magnitudes for the northeast and southwest extensions are equal to within a tenth of a magnitude, with $R = 20.0 \pm 0.5$ mag for each side. Again, the uncertainty depends on the PSF subtraction and scales upward or downward uniformly for both sides of the disk. To first order, both extensions have the same scattering cross section of dust, even though the spatial distribution is

[1] Astronomy Department, University of California, Berkeley, CA 94720; kalas@astron.berkeley.edu.
[2] National Science Foundation Center for Adaptive Optics, University of California, Santa Cruz, CA 95064.

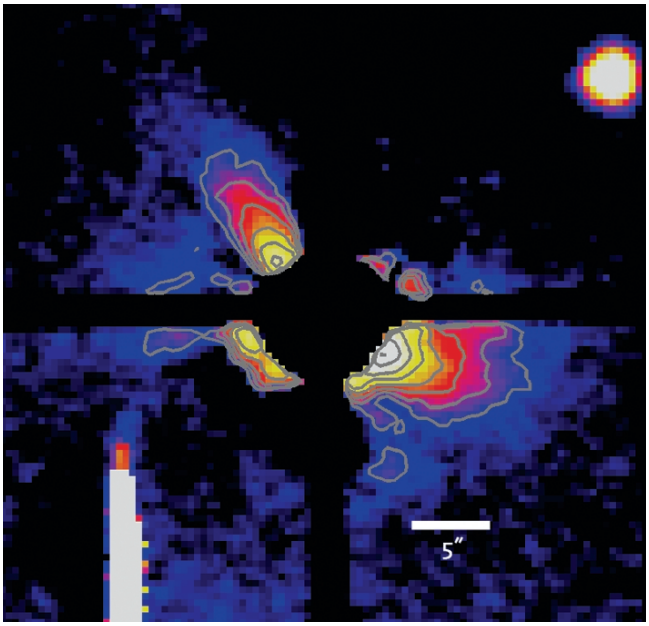

FIG. 1.—Coronagraphic *R*-band image of HD 32297 after PSF subtraction. Intensity is displayed on a logarithmic scale with false colors. Contours are spaced at intervals of 0.5 mag arcsec^{-2}, and the outer contour represents 23.5 mag arcsec^{-2}. North is up, east is left, and the field shown is 40″ × 40″. The bright column from the lower left is a saturation column on the CCD from the star BD +7 777s (V = 10.2, 47.″9 east and 78.″6 south of HD 32297). The dominant source of instrumental scattered light is from the bright star HD 32304 (V = 6.9, 61″ east and 134″ south of HD 32297).

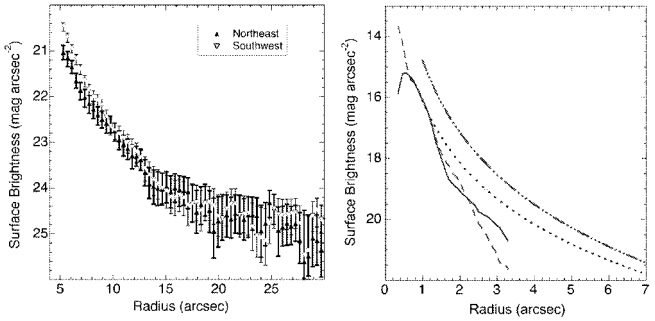

FIG. 2.—Midplane surface brightness as a function of radius for the northeast and southwest extension of HD 32297. *Left: R*-band surface brightness profile of a midplane cut with width 1.″2. Error bars indicate uncertainty from the subtraction of the PSF. The surface brightness profiles may be fit by power laws as described in the text. *Right:* Inward extrapolation of the *R*-band surface brightness profile represented by the power-law fits for comparison to the *HST* NICMOS F110W data. The *R*-band southwest disk midplane (*dash-dotted line*) and the northeast disk midplane (*dotted line*) are both brighter than the F110W midplanes detected by Schneider et al. (2005) (solid line is the northeast extension, dashed line is the southwest extension), consistent with a blue color for the nebulosity.

significantly different, similar to the findings for the β Pic disk (Kalas & Jewitt 1995).

Between 5″ and 15″ radius, the two midplane profiles can be described by power laws with indices -2.7 ± 0.2 and -3.1 ± 0.2 for the northeast and southwest sides, respectively (Fig. 2). These indices are comparable to the F110W surface brightness profile of the northeast midplane between 1.″6 and 3.″3 radius (Schneider et al. 2005). The similarity supports extrapolating the *R*-band surface brightness profile inward to estimate the $R -$ F110W disk color within 3.″3 radius (Fig. 2). We find $R -$ F110W ≈ -1 mag for the northeast extension and -2 mag for the southwest extension, whereas the intrinsic stellar color is $R -$ F110W $= +0.21$ mag. The blue scattered light color is consistent with submicron Raleigh scattering grains found in the interstellar medium (Draine 2003), as well as the outer region of the AU Mic debris disk (Metchev et al. 2005). If HD 32297 is comparable in spectral type to β Pic (A5 V), then grains with radii smaller than $\sim$5 μm will be blown out of the system on one dynamical timescale ($\sim 10^3$ yr; Artymowicz & Clampin 1997). Below we discuss how the presence of small grains ($\sim$0.1 μm) leads to several plausible scenarios for the origin of the nebulosity and the age of the system.

4. DISCUSSION

The asymmetric, large-scale morphology and the blue color of the nebulosity surrounding HD 32297 indicate that a population of dust grains may be primordial, originating from the interstellar medium. Interstellar grains have a size distribution that peaks at 0.1–0.2 μm (Kim et al. 1994; Mathis 1996) and many reflection nebulosities have a blue color (Witt & Schild 1986). However, the morphology of the HD 32297 nebulosity between 0.″5 and 1.″7 radius satisfies four criteria for the imaging detection of a circumstellar disk (Kalas & Jewitt 1997). In this inner region the disk is relatively symmetric, and a power-law fit to the surface brightness profile has index -3.6 (Schneider et al. 2005), which is comparable to the outer disk regions of β Pic and AU Mic (Kalas et al. 2004). The steepness of this surface brightness profile is consistent with models of an outward propagation of grains from an interior source region due to radiation pressure (Augereau et al. 2001). Beyond 1.″7 (190 AU) radius the disk may overlap with an interstellar nebulosity, or it may be influenced by forces that are otherwise insignificant in the inner disk.

If the large-scale nebulosity is produced by a random encounter between an A star and a clump of interstellar gas and dust, then the resulting morphology should demonstrate the signature linear filamentary features of the Pleiades phenomenon (Kalas et al. 2002). We do not detect Pleiades-like nebulosity, although interaction with the ISM is nevertheless plausible as the Galactic location of HD 32297 ($l = 192.^\circ83$, $b = -20.^\circ17$) coincides with a ridge of relatively high density gas outside of our Local bubble (Fig. 3; Kalas et al. 2002). This ridge also contains two stars surrounded by optical nebulosity that are members of the Pleiades open cluster (M45; $d = 118 \pm 4$ pc; van Leeuwen 1999). The proper motion vector of HD 32297 ($\mu_\alpha = 7$ mas yr^{-1}, $\mu_\delta = -23$ mas yr^{-1}) points to the south-southeast, with a sky-plane motion corresponding to 12.7 km s^{-1} at 112 pc distance. Therefore, the southern side of the disk will suffer enhanced erosion that would result in both a brighter nebulosity and diminished disk mass, compared to the northern side of the disk. Lissauer & Griffith (1989) refer to this process as ISM sandblasting, and Artymowicz & Clampin (1997) show that stellar radiation pressure would protect the circumstellar disk from the ISM up to a few hundred AU radius from the star. The ISM avoidance radius is a function of several factors, such as ISM density, relative velocity, and encounter geometry. A more detailed model applied specifically to HD 32297 is required to understand whether the observed disk asymmetries are consistent with ISM sandblasting. However, Artymowicz & Clampin (1997) cautioned that ISM grains do not have sufficient mass to perturb grains vertically away from a disk midplane. If this is valid, then other processes could create the observed *R*-band asymmetries, such as the entrainment of small grains by the ISM gas that should be associated with the ISM dust, or

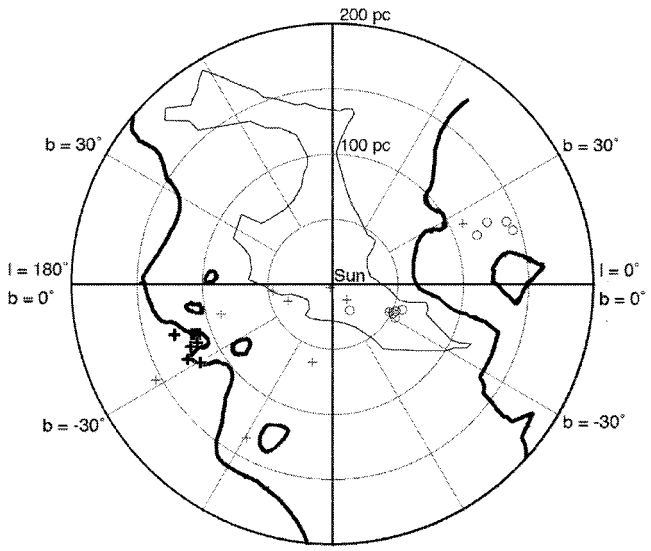

FIG. 3.—Association of HD 32297 with interstellar gas beyond the local bubble. HD 32297 is plotted with a filled square (*lower left quadrant*) in this figure adapted from Kalas et al. (2002) showing the spatial relationship between infrared excess stars and interstellar gas. This is the meridian plane of the Galaxy, containing both Galactic poles and the Galactic center to the right. Thin and thick contours represent neutral gas mapped by Sfeir et al. (1999) using the Na I D-line doublet. Other symbols on the map represent the location of stars that possess the far infrared signature of debris disks. Stars are mapped here if they have $l = 0° \pm 18°$ or $180° \pm 18°$. HD 32297 is therefore included in this plot, and appears superimposed on a wall or ridge of relatively dense interstellar gas (>50 mÅ D2-line equivalent width). Thick crosses mark five more stars that appear to trace the boundary of the wall, although the uncertainties in the *Hipparcos* parallaxes effectively place them at the same heliocentric distance. To the left of HD 32297 is HD 28149, and just below HD 32297 are 18 Tau (HD 23324) and 21 Tau (HD 23432), members of the Pleiades open cluster. Two more debris disk candidate stars along the bottom portion of this ridge are HD 28978 and HD 28375 (Backman & Paresce 1993). They lie closest to HD 32297 in Galactic latitude.

dynamical perturbations from the two stars, HD 32304 (G5, $d = 134^{+18}_{-15}$ pc) and BD +7 777s, south-southeast of HD 32297 (Figs. 1 and 4).

In the ISM sandblasting scenario, HD 32297 could be a main sequence star presently undergoing a random encounter with a clump of ISM. An alternate hypothesis is that HD 32297 is very young, and the nebulosity resembles that of SU Aur and Z CMa because the dust is the remnant of an outflow cavity, or more generally represents pristine matter from the natal cloud. The position angle discrepancies could arise because *HST* NICMOS is sensitive to the circumstellar disk at <200 AU radius with P.A. ≈ 48°, whereas our *R*-band data observe the top (out of the sky plane) of an outflow cavity associated with this inner disk. However, the lack of reddening ($V - K = 0.54$ mag, $J - H = 0.06$, $H - K = 0.03$) generally argues against a massive obscuring dust disk, such as that discovered around the Herbig Ae/Be Star PDS 144N (Perrin et al. 2006). Examination of several degrees of sky surrounding HD 32297 in the Digitized Sky Survey reveals filamentary nebulosities to the southeast and southwest, apparently associated with the λ Orionis molecular ring (Sh 2-264) to the east (Fig. 4). λ Orionis is in the background at ~400 pc, and its diameter is no greater than 20 pc in radius (Maddalena & Morris 1987; Dolan & Mathieu 2002). Therefore, HD 32297 must originate from a different star-forming region. Taurus-Aurigae, ~10° to the north of HD 32297 and with heliocentric distance 140 ± 20 pc (Elias 1978), may be a possibility. The proper motion of HD 32297 is comparable to T Tauri

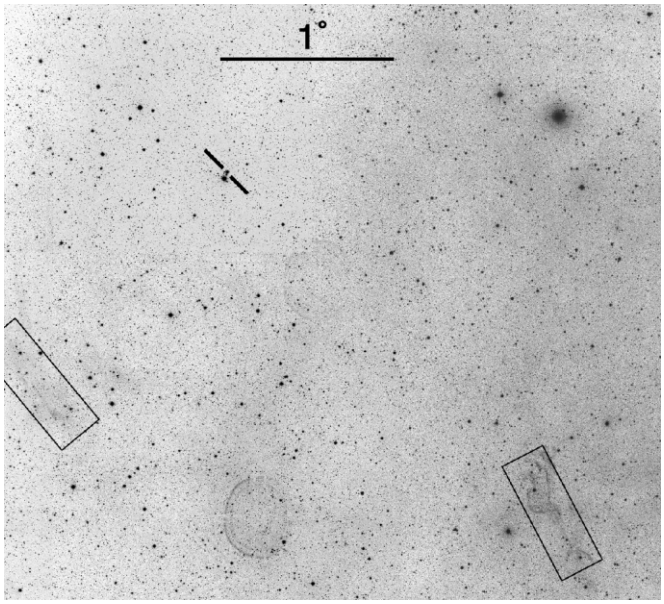

FIG. 4.—Digitized Sky Survey image of the region around HD 32297 (marked between diagonal lines) shows significant nebulosity in the large-scale environment (north is up, east is left). Filamentary Hα nebulosities on scales of tens of arcminutes (*rectangles*), are evident to the southeast (Sh 2-262) and southwest (Sh 2-260) of HD 32297. They are most likely associated with λ Orionis molecular ring (Sh 2-264) to the east. The age and origin of HD 32297 are enigmatic due to the superposition of objects in its environment that could be associated with λ Orionis, the Gould Belt, or the Taurus molecular cloud.

stars in this region (Frink et al. 1997), but it does not have a relative excess southward that would flag HD 32297 as a runaway star. Therefore, if HD 32297 is indeed a pre–main-sequence star, then it formed in relative isolation from Taurus-Aurigae within an outlying clump of the main molecular cloud.

The discovery of young stars south of Taurus led Neuhauser et al. (1997) through similar considerations when discussing the origin of their lithium-rich targets. In addition, they proposed two alternatives that may be applicable to HD 32297. First, they noted that the midplane of the Gould Belt, with age ~30 Myr, passes south of Taurus. In fact, HD 32297 is located within the Gould Belt midplane. Second, star formation in Taurus-Aurigae may have been triggered 30 Myr ago when a high-velocity cloud passed northward through the Galactic plane (Lepine & Duvert 1994). The first generation of stars formed at this earlier epoch within the molecular cloud, which eventually passed again southward through the Galactic plane. The second passage formed a new generation of stars observed today in Taurus-Aurigae, with the first generation separating from the natal material when the latter decelerated as it encountered denser ISM in the Galactic plane. The first-generation stars are currently found south of Taurus (both in Galactic latitude and declination). Therefore, whether associated with the Gould Belt or with Taurus-Aurigae, the young stars currently located south of the Taurus molecular cloud have age ~30 Myr. HD 32297 may be a member of either group given that the relatively large dust disk surrounding it may be adopted as a proxy for spectroscopic youth indicators.

5. CONCLUSIONS AND FUTURE WORK

Coronagraphic *R*-band data reveal that the circumstellar nebulosity surrounding HD 32297 is significantly distorted relative to the near edge-on disk observed within 400 AU with *HST* NICMOS. We detect nebulosity as far as 1680 AU radius, with long axes that deviate from the NICMOS position angles by

~15° for each midplane. The southwest midplane is warped and vertically distended. We invoke the possibility of ISM sandblasting, which is consistent with the southward proper motion of HD 32297. We examine several scenarios relating to the age and origin of HD 32297. Association with either the Gould Belt or Taurus-Aurigae would give age ~30 Myr, similar to that of β Pic. A younger age is also possible if HD 32297 formed in an isolated, outlying cloud of Taurus-Aurigae.

If the ISM sandblasting scenario is correct, then future multicolor imaging should reveal significant color differences between the northeast and southwest sides of the disk. The southwest side may also show significant color structure perpendicular to disk midplane if the apparent distortions in the disk are due to small grains swept northward. Dynamical perturbations are possible if either HD 32304 or BD +7 777s to the southeast are physically associated with HD 32297. Future spectroscopic observations of HD 32297 should also include these two stars to constrain their spectral types, relative motions, and ages. If the radial velocities support a physical association, then either HD 32304 or BD +7 777s may demonstrate additional age indicators that would constrain the evolutionary status of HD 32297. Moreover, if HD 32297 is a β Pic analog, then multiepoch spectroscopy should test for the variable, transient redshifted features thought to arise from cometary activity under the dynamical influence of planets (Beust & Morbidelli 2000).

This work was supported in part by NASA grants to P. K., and by the NSF Center for Adaptive Optics, managed by the University of California, Santa Cruz, under cooperative agreement AST 98-76783. We thank Michael Ratner (SAO/Harvard) for supporting the observing campaigns at the University of Hawaii 2.2 m telescope.

REFERENCES

Artymowicz, P., & Clampin, M. 1997, ApJ, 490, 863
Augereau, J. C., Nelson, R. P., Lagrange, A. M., Papaloizou, J. C. B., & Mouillet, D. 2001, A&A, 370, 447
Backman, D. E., & Paresce, F. 1993, in Protostars and Planets III, ed. E. H. Levy & J. I. Lunine (Tucson: Univ. Arizona Press), 1253
Beust, H., & Morbidelli, A. 2000, Icarus, 143, 170
Dolan, C. J., & Mathieu, R. D. 2002, AJ, 123, 387
Draine, B. T. 2003, ARA&A, 41, 241
Elias, J. H. 1978, ApJ, 224, 857
Frink, S., Roser, S., Neuhauser, R., & Sterzik, M. F. 1997, A&A, 325, 613
Kalas, P., Graham, J. R., Beckwith, S. V. W., Jewitt, D., & Lloyd, J. P. 2002, ApJ, 567, 999
Kalas, P., & Jewitt, D. 1995, AJ, 110, 794
———. 1996, AJ, 111, 1347
———. 1997, Nature, 386, 52
Kalas, P., Liu, M. C., & Matthews, B. C. 2004, Science, 303, 1990
Kim, S.-H., Martin, P. G., & Hendry, P. D. 1994, ApJ, 422, 164
Lepine, J. R. D., & Duvert, G. 1994, A&A, 286, 60
Lissauer, J. J., & Griffith, C. A. 1989, ApJ, 340, 468
Maddalena, R. J., & Morris, M. 1987, ApJ, 323, 179
Mathis, J. S. 1996, ApJ, 472, 643
Metchev, S. A., Eisner, J. A., Hillenbrand, L. A., & Wolf, S. 2005, ApJ, 622, 451
Nakajima, T., & Golimowski, D. A. 1995, AJ, 109, 1181
Neuhauser, R., Torres, G., Sterzik, M. F., & Randich, S. 1997, A&A, 325, 647
Perrin, M. D., Duchene, G., Kalas, P., & Graham, J. R. 2006, ApJ, submitted
Schneider, G., Silverstone, M. D., & Hines, D. C. 2005, ApJ, 629, L117
Sfeir, D. M., Lallement, R., Crifo, F., & Welsh, B. Y. 1999, A&A, 346, 785
Smith, B. A., & Terrile, R. J. 1984, Science, 226, 1421
van Leeuwen, F. 1999, A&A, 341, L71
Witt, A. N., & Schild, R. E. 1986, ApJS, 62, 839